Convergence of highly parallel stray field calculation using the fast multipole method on irregular meshes

Cite as: AIP Advances **8**, 056019 (2018); https://doi.org/10.1063/1.5006896
Submitted: 28 September 2017 . Accepted: 10 November 2017 . Published Online: 28 December 2017

P. Palmesi, C. Abert, F. Bruckner, and D. Suess

Convergence of highly parallel stray field calculation using the fast multipole method on irregular meshes

P. Palmesi,[a] C. Abert, F. Bruckner, and D. Suess
Faculty of Physics, University of Vienna, Vienna, Austria

(Presented 10 November 2017; received 28 September 2017; accepted 10 November 2017; published online 28 December 2017)

Fast stray field calculation is commonly considered of great importance for micromagnetic simulations, since it is the most time consuming part of the simulation. The Fast Multipole Method (FMM) has displayed linear $O(N)$ parallelization behavior on many cores. This article investigates the error of a recent FMM approach approximating sources using linear—instead of constant—finite elements in the singular integral for calculating the stray field and the corresponding potential. After measuring performance in an earlier manuscript, this manuscript investigates the convergence of the relative L^2 error for several FMM simulation parameters. Various scenarios either calculating the stray field directly or via potential are discussed.
https://doi.org/10.1063/1.5006896

INTRODUCTION

Every distributed computational solution to the laplace equation—in this case the stray field—has to deal with its bad scalability properties. The fast multipole method has been shown to exhibit high parallel efficiency (> 70%) across thousands of cores in memory and time[1]—albeit for a point like Laplace kernel.

To achieve its superior performance the FMM approximates the discretized problem by using multipole and local expansions. While an upper limit for the error can be theoretically computed no actual error data has been published, making it hard to determine applicability of FMM, choosing a suiting implementation and verifying the correct implementation. This work compares the error of two different implementations.

The direct stray field solution of potential or field is required for a whole class of algorithms including FMM, non uniform grid, fast Fourier transform and the tensor grid method, making this publication a reference for the implementation of all of the mentioned algorithms.[2]

METHODS

The presented FMM implementation is a modified version of a previously published algorithm.[2] The FMM splits the problem into two parts. An analytic near- or direct field and a multipole approximation for the far-field. The changes to the original implementation are primarily the separate calculation of volume and surface terms (see below) and the direct calculation of the stray field in addition to the corresponding potential. This manuscript is mainly concerned with the errors introduced by the FMM and discretization of the problem.

All simulations in this manuscript were computed on a quad-core workstation with 3.2 GHz clock frequency.

[a]Corresponding author: palmesip85@univie.ac.at

Stray field problem and discretization

Following equations solve the stray field problem, Equation (2) was used for the calculation of the potential:

$$u(\boldsymbol{r}) = -\frac{1}{4\pi}\int_{\Omega} \boldsymbol{M}(\boldsymbol{r}') \cdot \nabla' \frac{1}{|\boldsymbol{r}-\boldsymbol{r}'|} \mathrm{d}\boldsymbol{r}' \tag{1}$$

$$u(\boldsymbol{r}) = \frac{1}{4\pi}\left[\int_{\Omega} \frac{\nabla' \cdot \boldsymbol{M}(\boldsymbol{r}')}{|\boldsymbol{r}-\boldsymbol{r}'|} \mathrm{d}\boldsymbol{r}' - \int_{\partial\Omega} \frac{\boldsymbol{M}(\boldsymbol{r}') \cdot \boldsymbol{n}(\boldsymbol{r}')}{|\boldsymbol{r}-\boldsymbol{r}'|} \mathrm{d}\boldsymbol{r}'\right] \tag{2}$$

Equation (3) was used to calculate the field:

$$\boldsymbol{H}_D(\boldsymbol{r}) = -\nabla u(\boldsymbol{r})$$

$$\boldsymbol{H}_{\mathrm{D}}(\boldsymbol{r}) = -\frac{1}{4\pi}\left[\int_{\Omega} \nabla' \cdot \boldsymbol{M}(\boldsymbol{r}') \nabla \frac{1}{|\boldsymbol{r}-\boldsymbol{r}'|} \mathrm{d}\boldsymbol{r}' - \int_{\partial\Omega} \boldsymbol{M}(\boldsymbol{r}') \cdot \boldsymbol{n}(\boldsymbol{r}') \nabla \frac{1}{|\boldsymbol{r}-\boldsymbol{r}'|} \mathrm{d}\boldsymbol{r}'\right] \tag{3}$$

Both the sources $\boldsymbol{M}$ and the solution u are discretized with piecewise affine, globally continuous functions based on a nodal basis of hat functions $\phi_i(\boldsymbol{r}_j) = \delta_{i,\,j}$ with i, j denoting the nodes of a tetrahedral mesh. This naturally leads to cell-wise constant globally discontinuous discretization of the field $\boldsymbol{H}_{\mathrm{D}}$ (see Figure 1) calculated at the cell centers to avoid diverging fields at the nodes.

In Palmesi *et al.*[2] Equation (1) has been solved directly for each cell using Graglia,[3] leading to—potentially large—canceling surface contributions inside the mesh. The multipole error is dependent on the absolute value of the integral Equation (1) making the direct solution suboptimal. In Equations (2) and (3) field and potential have been split into surface $\partial\Omega_i$ and volume Ω_i terms forgoing this problem.[2] The modified version used here requires six new subprograms. Four calculate the analytic surface and volume contributions of resp. field and potential and two calculate the expansion of surface and volume contributions which are identical for field and potential.

Fast multipole method

The FMM[4] divides the mesh into two hierarchic tree data structures. The source tree and the target tree (see Figure 1). Each branch has a center, a radius (r_t/r_s) that spans the geometric region of its children and a multipole moment Q or L. Starting at the roots, the θ-criterion ($\theta > (r_s + r_t)/R$; Figure 1) determines which target branches interact with a source branch via multipole expansion. The remaining branches are recursively checked, or—at the leaf level—the interaction is computed directly. The multipole expansion is cut off at the maximum multipole order P. A detailed description of the modified expansion terms and the implementation of the analytic calculation[3,5] will follow in a later publication.

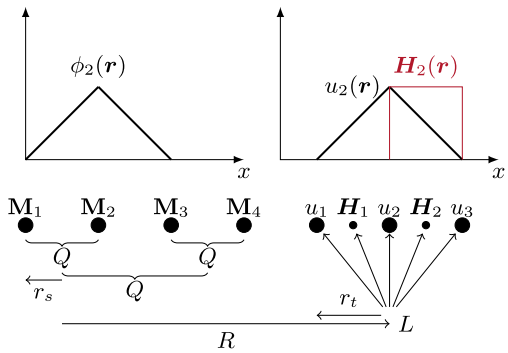

FIG. 1. The discretization was done using a tetrahedral mesh with hat-functions. M_i and u_i are defined node-wise; H_i cell-wise. The FMM combines magnetizations to multipole moments Q in the source tree which are transformed into local expansions L in the target tree. The source radii r_s, target radii r_t and distance R are used for the θ-criterion $\theta > \frac{r_s+r_t}{R}$ (see section fast multipole method).

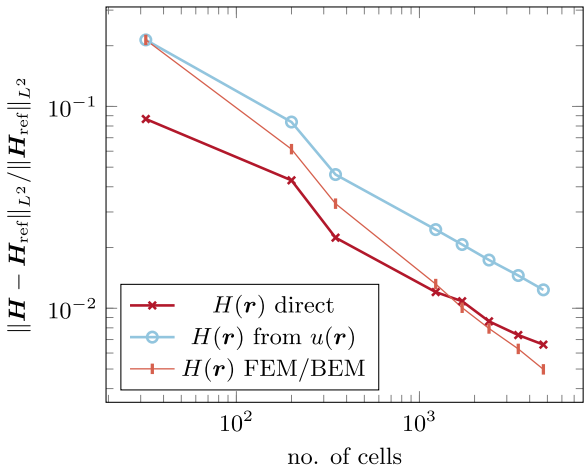

FIG. 2. $\|\boldsymbol{H}_{\text{D}} - \boldsymbol{H}_{\text{ref}}\|_{L^2} / \|\boldsymbol{H}_{\text{ref}}\|_{L^2}$ error on a sphere mesh for discretized calculation of field(discretization) or via direct potential and FEM/BEM simulation. $\boldsymbol{H}_{\text{ref}}$ is the analytic solution of the ideal sphere.

RESULTS

The discretization error without FMM was calculated using a homogeneously magnetized unit-sphere (Figure 2) and unit-cube mesh (Figure 3). The reference field $\boldsymbol{H}_{\text{ref}}$ was calculated analytically for an ideal geometric sphere to be $H_x = H_y = 0; H_z = -\frac{1}{3} m_S$ and for the cube using reference Akoun and Yonnet.[6] The discretization error used is the euclidean norm $\|(\boldsymbol{H}_{\text{D}} - \boldsymbol{H}_{\text{ref}}\|_{L^2} / \|\boldsymbol{H}_{\text{ref}}\|_{L^2}$. The potential solution was differentiated cell-wise for comparison.

Figure 2 shows how the discretization error decreases exponentially with increasing degrees of freedom (DOF) of the sphere mesh. It allows to compare the error caused by using fewer DOFs i.e. potential versus field. Figure 3 shows the same error for a regular cube mesh exhibiting a similar exponential decrease in error. The field discretization error is not plotted because it is zero.

Figure 4 shows the normalized, spatially averaged magnetization path over time for the standard problem 4(SP4) with switching field 1.[7] The initial S-state was calculated by FEM/BEM providing an identical starting point for the simulation. The mesh discretization was done using dolfin's[8] *BoxMesh* using a discretization of (100,25,1) along the respective (x,y,z)-axes. Both paths show the expected switching behavior confirmed by the FEM/BEM reference solution. They are reused as FMM error references below.

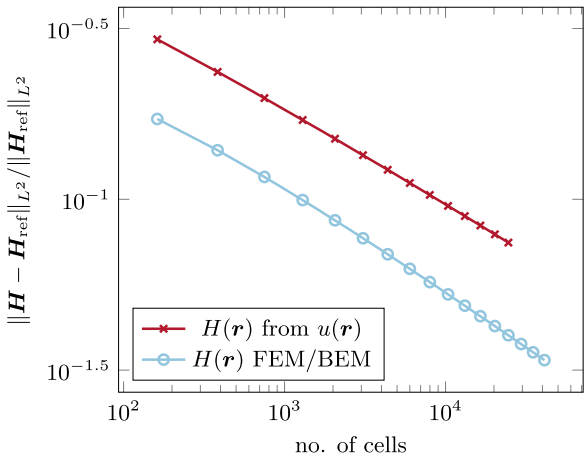

FIG. 3. $\|\boldsymbol{H}_{\text{D}} - \boldsymbol{H}_{\text{ref}}\|_{L^2} / \|\boldsymbol{H}_{\text{ref}}\|_{L^2}$, error on a cube (constant magnetization in z-direction $m_z = 1$) for discretized calculation of field, via potential and FEM/BEM simulation. $\boldsymbol{H}_{\text{ref}}$ is the analytic solution of the cube.[6]

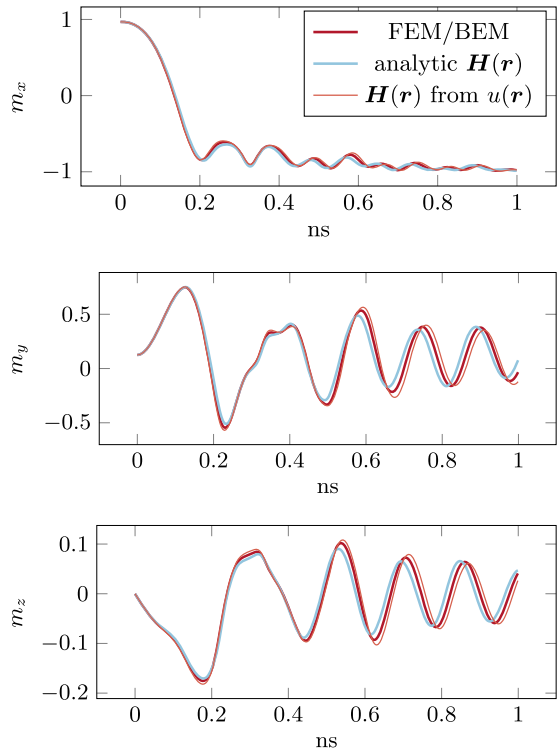

FIG. 4. Comparison of the magnetization in x-,y- and z-direction for the standard problem 4[7] using a higher order preconditioned BDF scheme.[9]

FMM error evaluation

The FMM error $\|(x - x_{\text{ref}})\|_{L^2}\|/\|x_{\text{ref}}\|_{L^2}$ was computed using x as potential $u(\boldsymbol{r})$ or field $\boldsymbol{H}_{\text{D}}(\boldsymbol{r})$ for the S-state of the standard problem 4 with various simulation parameters as multipole acceptance criterion[2] θ and maximum multipole expansion order[2] P. The potential was compared to the direct (reference) solution from Figure 4 to show the error introduced by the FMM without the discretization error. The maximum leaf element count for the tree (ncrit)[10] was set to 8.

The performance in Table I is not fully optimized yet; timings should not be seen as the maximum possible performance. Compare Palmesi *et al.*[2] for a deeper performance analysis.

DISCUSSION

Figures 2 and 3 show a decreasing error for larger meshes. The error estimates might seem large but the error in energy is much lower, as seen by the correct behavior for the SP4 in Figure 4. The field error was chosen to make it directly comparable to the errors introduced by the FMM in Figures 5 and 6.

Figures 5 and 6 exhibit similar error regimes for equal FMM parameters θ and P. The expected exponential behavior proportional to θ^P can be observed. θ and P determine the performance of the

TABLE I. Timings (ms) for FMM calculation with maximum expansion order P and θ-criterion for SP4.

	θ for u					θ for $\boldsymbol{H}_D$				
P	0.3	0.4	0.5	0.6	0.7	0.3	0.4	0.5	0.6	0.7
3	205	134	96	73	57	217	140	101	78	59
4	280	185	134	100	78	293	198	139	107	81
5	454	300	219	167	131	468	313	226	171	139
6	725	481	350	269	208	803	500	367	281	219

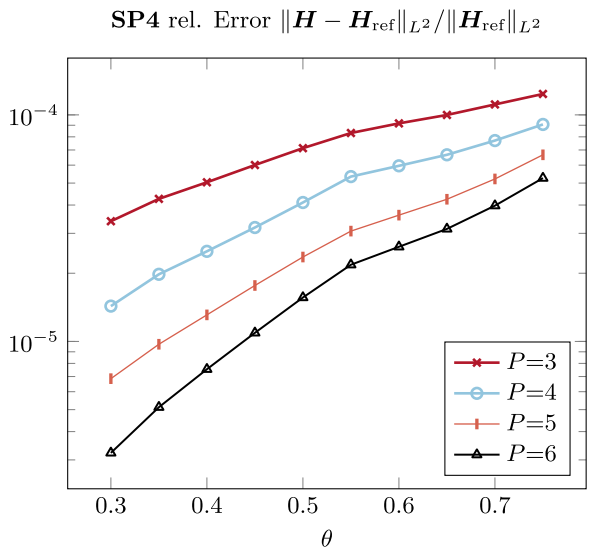

FIG. 5. FMM error convergence for SP4 in the S-state for various multipole acceptance criteria θ and multipole order P.

algorithm. The number of direct interaction and Q to L transformation show a non-trivial inverse relationship with θ depending on the problem geometry. The far-field performance is $O(P^3)$ because of the $P * (P + 1) * (P + 2)/6$ coefficients at maximum order P. An optimal combination of θ and P for a given solution can be found by benchmarking the results.

To find the optimal algorithm following thoughts should be considered. Preliminary results show that the error caused by the potential discretization is largest at the corners and edges of the mesh. This means that for simulations where the L^2 error or energy are important the potential is a good candidate *but* if a correct field near the mesh boundaries is necessary the direct field calculation should be used instead. If an averaged field is necessary a different method should be considered.[11] By using the potential a third of the computation cost can be saved in the near-field. The far-field calculation can be achieved by virtually the same time and code for field and potential.

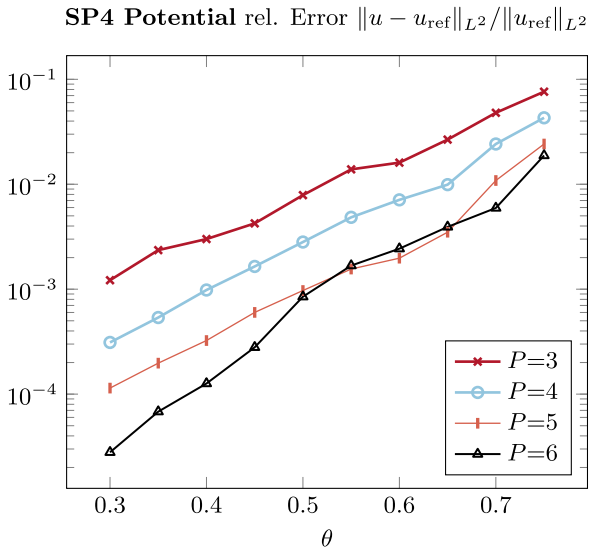

FIG. 6. FMM error convergence for SP4 via potential in the S-state for various multipole acceptance criteria θ and multipole order P.

In summary it can be said, that an error of a few percent in the energy can be achieved with simulation parameters like $P = 4$ and $\theta = 0.6$ or even $P = 3$ making the presented FMM a scalable and accurate method for fast parallel stray field calculation on irregular meshes.

ACKNOWLEDGMENTS

The authors acknowledge the CD-Laboratory AMSEN (financed by the Austrian Federal Ministry of Economy, Family and Youth, the National Foundation for Research, Technology and Development) for financial support.

[1] R. Yokota and L. A. Barba, International Journal of High Performance Computing Applications **26**, 337 (2012), 29.
[2] P. Palmesi, L. Exl, F. Bruckner, C. Abert, and D. Suess, Journal of Magnetism and Magnetic Materials **442**, 409 (2017).
[3] R. Graglia, IEEE Transactions on Antennas and Propagation **35**, 662 (1987), 23.
[4] L. Greengard and V. Rokhlin, Journal of Computational Physics **73**, 325 (1987), 15.
[5] M. Rech, "Effiziente Nahfeldkubatur in der Galerkin-Randelementmethode," Ph.D. thesis, Rheinische Friedrich-Wilhelms-Universität Bonn (2002).
[6] G. Akoun and J. P. Yonnet, IEEE Transactions on Magnetics **20**, 1962 (1984).
[7] R. D. McMichael, M. J. Donahue, D. G. Porter, and J. Eicke, Journal of Applied Physics **89**, 7603 (2001).
[8] A. Logg and G. N. Wells, ACM Trans. Math. Softw. **37**(20), 1 (2010).
[9] D. Suess, V. Tsiantos, T. Schrefl, J. Fidler, W. Scholz, H. Forster, R. Dittrich, and J. J. Miles, Journal of Magnetism and Magnetic Materials **248**, 298 (2002).
[10] R. Yokota, D. Koyama, C.-H. Lai, and N. Yamamoto, Journal of Algorithms & Computational Technology **7**, 301 (2013), 18.
[11] D. Chernyshenko and H. Fangohr, Journal of Magnetism and Magnetic Materials **412**, 132 (2016), 24.